BIOCELL
2024 48(6): 991-999
ARTICLE

Tech Science Press

Bhlhe40 protects cochlear hair cell-like HEI-OC1 cells against H_2O_2-triggered oxidative injury

Liting WEN[#]; Xiaoxia ZENG[#]; Peixiong CHEN; Dapeng ZHAO; Yangyang LI; Xianhai ZENG[*]

Department of Otorhinolaryngology, Longgang Otorhinolaryngology Hospital and Shenzhen Key Laboratory of Otorhinolaryngology, Shenzhen Institute of Otorhinolaryngology, Shenzhen, China

Key words: *Bhlhe40*, Oxidative injury, Cochlear hair cell, Histone deacetylases 2

Abstract: Background: Cochlear hair cell injury is a common pathological feature of hearing loss. The basic helix-loop-helix family, member e40 (*Bhlhe40*), a gene belonging to the basic helix-loop-helix (bHLH) family, exhibits strong transcriptional repression activity. **Methods:** Oxidative damage, in House Ear Institute-Organ of Corti 1 (HEI-OC1) cells, was caused using hydrogen peroxide (H_2O_2). The Ad-*Bhlhe40* particles were constructed to overexpress *Bhlhe40* in HEI-OC1 cells. Various assays including cell counting kit-8 (CCK-8), terminal deoxynucleotidyl transferase-mediated dUTP nick end-labeling assay (TUNEL), flow cytometry, immunofluorescence, and corresponding commercial kits were employed to investigate the impacts of *Bhlhe40* on cell viability, apoptosis, oxidative stress levels, mitochondrial membrane potential and cellular senescence. Additionally, a dual-luciferase reporter assay was performed to confirm the targeting of the histone deacetylases 2 (*Hdac2*) by *Bhlhe40*. **Results:** The results revealed that *Bhlhe40* was downregulated in H_2O_2-treated HEI-OC1 cells, but its overexpression improved cell viability and mitigated H_2O_2-induced oxidative injury in HEI-OC1 cells with increase of superoxide dismutase (SOD), catalase (CAT) and glutathione peroxidase (GPx) activities and decrease of reactive oxygen species (ROS) levels. Besides, overexpression of *Bhlhe40* suppressed H_2O_2-triggered cell senescence, as evidenced by the fact that the upregulation of P53, P21, and P16 in HEI-OC1 cells treated with H_2O_2 were all alleviated by *Bhlhe40* overexpression. And we further verified that overexpression of *Bhlhe40* could inhibit the expression of *Hdac2*, which may be related to the repression of *Hdac2* transcription. **Conclusion:** This study suggests that *Bhlhe40* plays a protective role against senescence and oxidative damage in cochlear hair cells exposed to H_2O_2.

Introduction

Cochlear hair cells are a crucial population of sensory cells in the spiral organ of Corti, responsible for detecting sound waves. And these cells are highly susceptible to the environmental factors like exposure to loud noises or certain medications, as well as genetic factors that may contribute to hearing loss [1,2]. Recent research indicates that cochlear hair cell injury is a significant causative contributing factor to the development of sustained noise-induced hearing loss [3]. Following exposure to traumatic noise, cochlear hair cells experience massive accumulation of free radicals and reactive oxygen species (ROS) [4], leading to oxidative stress and subsequent cellular damage that affects various cellular processes such as cell proliferation, apoptosis and senescence [5]. The cascading effects of oxidative stress induced by ROS have been linked to cochlear damage [6], specifically through the activation of the caspase-mediated apoptosis pathway leading to hair cell loss [7]. Experimental exposure of cells to hydrogen peroxide (H_2O_2) increases ROS levels [8], and exposure of House Ear Institute-Organ of Corti 1 (HEI-OC1) cells to H_2O_2 usually serve as a model to study oxidative stress-induced damage [9]. Currently, antioxidant treatment has shown promise in mitigating redox imbalances and preventing sensory hair cell death in the cochlea [10,11].

The basic helix-loop-helix family, member e40 (*Bhlhe40*) is a basic helix-loop-helix (bHLH) gene known for its transcriptional repression activity through the alpha-helix rich domain in its C terminus [12,13]. Studies have demonstrated that *Bhlhe40* is ubiquitously expressed in mammalian tissues [14] and plays a pivotal role in

*Address correspondence to: Xianhai Zeng, zxhklwx@163.com
[#]The authors contributed equally to this research
Received: 31 January 2024; Accepted: 21 March 2024;
Published: 10 June 2024

neurogenesis, immune regulation, and apoptosis [15,16]. Notably, *Bhlhe40* has been implicated in diseases associated with oxidative stress, with its deficiency leading to signs of oxidative stress and muscle death in mice [17]. Conversely, overexpression of *Bhlhe40* enhanced the resistance of podocytes to ROS-induced injury [18]. ROS and its byproducts are well-documented in disrupting the internal connections of molecules, potentially causing damage to cochlear cells or tissues and resulting in hearing loss [3,19]. However, to date, there has been no reported information on whether and how *Bhlhe40* contributes to oxidative stress-induced injury in cochlear hair cell.

Additionally, *Bhlhe40* has been associated with the regulation of histone deacetylase (*Hdac*) [20]. Studies have shown decreased levels of histone acetylation and increased levels of histone deacetylases 1, 2, and 3 (*Hdac1*, *Hdac2* and *Hdac3*) in the cochlear cells of adult mice following exposure to traumatic noise [21]. Given the transcriptional repression function of *Bhlhe40*, we hypothesize that *Bhlhe40* may be involved in the oxidative injury of cochlear hair cells by modulating the transcription of *Hdac*.

This study aims to explore the impacts of *Bhlhe40* on an H_2O_2-induced oxidative injury model in cochlear hair cells and elucidate its underlying mechanism.

Materials and Methods

Cell culture

HEI-OC1 cells (M8-0401, OriCell, Guangzhou, China), a mouse auditory cell line, were utilized in this study as an *in vitro* system to assess the functional response of *Bhlhe40* in oxidative injury to cochlear hair cells. Following a publicly available protocol in Journal of Visualized Experiments (JOVE; http://www.jove.com/) [9,22], HEI-OC1 cells were cultured in the Dulbecco's Modified Eagle's Medium (DMEM; G4510, servicebio, Wuhan, China), supplemented with 10% fetal bovine serum (FBS, 11011-8611, Tianhang, Huzhou, China) in the absence of antibiotics, and maintained at 33°C with 10% CO_2.

Adenovirus transduction

To construct the indicated recombinant adenovirus, the protein-coding DNA sequence (CDS) of *Bhlhe40* (NM_011498) was cloned into the shuttle plasmid pDC315 (VT1500, YouBio, Hunan, China) by Auhui General Biology (Chuzhou, China). The recombinant plasmid pDC315, containing *Bhlhe40*-CDS, was generated by digesting the pDC315 plasmid with Nhel and Sa1I enzymes. HEK-293A cells were then co-transfected with the *Bhlhe40*-pDC315 plasmid and the adenovirus helper plasmid as per the manufacturer's instructions to produce purified *Bhlhe40*-adenovirus (Ad-*Bhlhe40*) particles. Subsequently, HEI-OC1 cells were infected with Ad-*Bhlhe40* particles to achieve *Bhlhe40* overexpression.

Detection of cell viability

HEI-OC1 cells were plated at a density of 4×10^3/mL in a 96-well plate (5×10^3 cells/well) and exposed to 2 mM H_2O_2 for 4, 8 or 12 h in a 33°C incubator with 10% CO_2. Following this exposure, the cells were subjected to cell counting kit-8 solution (CCK-8; KGA317, KeyGen Biotech, Nanjing, China) for 2 h at a volume of 10 μL per well. Cell viability was then assessed by measuring the absorbance at 450 nm using a BioTek® 800™ TS Absorbance Reader (BioTek, USA).

RNA extraction and real-time polymerase chain reaction (real-time PCR)

TRIpure reagent (RP1001, BioTeke, Beijing, China) was utilized for total RNA extraction as per the manufacturer's instructions. The cDNA synthesis was carried out with M-MLV reverse transcriptase (D7160L, Beyotime, Shanghai, China) following the manufacturer's guidelines. Real-time fluorescence quantitative PCR was conducted on ExicyclerTM 96 (Bioneer, Korea) using SYBR Green (SY1020, Solarbio, Beijing, China) and 2 × Taq PCR MasterMix (PC1150, Solarbio, Beijing, China). β-actin served as a housekeeping gene. The relative expression of *Bhlhe40*, *Hdac1*, *Hdac2* and *Hdac3* were calculated based on $2^{-\triangle\triangle CT}$ method. The PCR primers are provided as follows:

Mus Bhlhe40 forward primer (FP), *AACGGAGCGAAG ACAGC*; reverse primer (RP), *CCAAGTGACCCAAAG TAGTAAG*.

Mus Hdac1 FP, *GGGCACCAAGAGGAAAG*; RP, *GCGA ATAGAACGCAGGA*.

Mus Hdac2 FP, *TTTTGGACCAGACTTCA*; RP, *CTAC GACCTCCTTCACC*.

Mus Hdac3 FP, *ATGTATGAAGTTGGAGCAG*; RP, *TTT CGGACAGTGTAGCC*.

Western blotting

Cells were lysed using RIPA lysis buffer (PR20001, Proteintech Group, Inc., Wuhan China) mixed with 1% protease inhibitor (PR20032, Proteintech Group, Inc., Wuhan, China). The lysate was then centrifuged at 10000 g for 3 min at 4°C to collect resulting supernatant. The concentration of protein was estimated using BCA Protein Concentration Assay Kit (PK10026, Proteintech Group, Inc., Wuhan, China). Samples containing 15–30 μg of proteins were loaded into each well and underwent sodium dodecyl sulfate-polyacrylamide gel electrophoresis. The proteins were subsequently transferred to a polyvinylidene fluoride membrane (LC2005, Thermo Scientific, Pittsburgh, PA, USA) and blocked with 5% skimmed milk in Tris-buffer-saline with Tween-20 buffer (TBST; PR20011, Proteintech Group, Inc., Wuhan, China). Protein expression levels were assessed following incubation with primary and secondary antibodies. Specifically, the membranes were probed overnight at 4°C with primary antibodies against BHLHE40 (1: 1000; 17895-1-AP, Proteintech Group, Inc., Wuhan, China), P53 (1: 1000; A0263, ABclonal Technology, Shanghai, China), P21 (1: 1000; A1483, ABclonal Technology, Shanghai, China), P16 (1: 1000; 10883-1-AP, Proteintech Group, Inc., Wuhan, China), Hdac2 (1: 1000; A2084, ABclonal Technology, Shanghai, China) or β-actin (1: 20000; 66009-1-Ig, Proteintech Group, Inc., Wuhan, China). After washing with Western Blot Liquid Detergent (PR20012, Proteintech Group, Inc., Wuhan, China), the

membranes were then incubated with the appropriate secondary antibodies HRP-conjugated Affinipure Goat Anti-Rabbit IgG (1: 10000; H + L, SA00001-2, Proteintech Group, Inc., Wuhan, China) or HRP-conjugated Affinipure Goat Anti-Mouse IgG (1: 10000; H + L, SA00001-1, Proteintech Group, Inc., Wuhan, China) for 40 min at 37°C. Following thorough rinsing of the membranes, the immune-reactive bands were visualized utilizing the Hypersensitive ECL Chemiluminescence Detection Kit (PK10003, Proteintech Group, Inc., Rosemont, IL, USA). The density value of bands were analyzed with the Gel-Pro-Analyzer software (Version 4.0, Media Cybernetics, Maryland, USA).

Detection of apoptosis

The AnnexinV-FITC Kit (KGA106, Nanjing, China) from KeyGen Biotech was utilized to quantify cell apoptosis. The indicated cells were initially plated in 6-well plates at a density of 5×10^5 cells per well and then exposed to 2 mM H_2O_2 for 4, 8 or 12 h. Subsequent to centrifugation at 150 g for 5 min, the supernatant was removed, and the cells were washed twice with PBS before being resuspended in 500 μL of binding buffer. Finally, the cells were incubated with Annexin V-FITC/PropidiumIodide (PI) staining reagent for 15 min at room temperature. The apoptotic cell percentage were determined using a flow cytometer (NovoCyte, Agilent, USA).

Terminal deoxynucleotidyl transferase-mediated dUTP nick end-labeling (TUNEL) assay

Apoptosis in HEI-OC1 cells was evaluate by analyzing DNA fragmentation using an *In Situ* Cell Death Detection Kit (12156792910, Roche, Basel, Switzerland) following the manufacturer's guidelines. The cell sections were stained with DAPI solution (D106471, Aladdin, Shanghai, China) for 5 min (protected from light) to visualize the cell nucleus. Following rinsing with PBS, the images were captured using a microscope (BX53, OLYMPUS, Japan).

Quantification of caspase-3

Apoptosis was assessed by measuring the activity of Caspase-3 in cell culture extracts with the Caspase-3 Activity Detection Kit (C1116, Beyotime, Shanghai, China) as per the manufacturer's protocol. Based on Caspase-3 catalyze the production of pNA (p-nitroaniline, yellow) from the substrate Ac-DEVD-pNA, Caspase-3 activity was assessed by measuring the absorbance of pNA at 405 nm.

ROS detection

The ROS Assay Kit (KGAF019) from KeyGen Biotech in Nanjing, China utilized the red fluorescent probe dihydroethidium (DHE) to evaluate cytosolic superoxide production. Specifically, after 48 h of adenovirus infection, cells were exposed to 2 mM H_2O_2 for 8 h. Afterward, the cell culture medium was aspirated, and the cells were incubated with 10 μM of DHE probe at 37°C for 30 min in the absence of light. To ensure the elimination of any residual DHE outside the cells, the incubated cells underwent three washes with serum-free cell culture medium. Finally, the cells were observed under an Olympus DP73 microscopic photography system (OLYMPUS, Tokyo, Japan).

Evaluation the activities of superoxide dismutase (SOD), catalase (CAT) and glutathione peroxidase (GPx)

Cell precipitates were resuspended in PBS and lysed through sonication. The protein content determination was carried out using a BCA protein assay kit (P0011, Beyotime, Shanghai, China). SOD (A001), CAT (A007) and GPx (A005) detection were performed with assay kits from Nanjing Jiancheng Bioengineering Institute (Nanjing, China) following the manufacturer's experimental procedure. The optical density (OD) readings were taken at 550 nm for SOD activity, 405 nm for CAT activity, and 412 nm for GPx activity using a UV-Vis spectrophotometer (UV752N, Shanghai Youke Instrument and Meter Co., Ltd., Shanghai, China).

Mitochondrial membrane potential (ΔΨm) detection

JC-1 Mitochondrial Membrane Potential Assay Kit (C2006, Beyotime, Shanghai, China) was employed to determine the ΔΨm in mitochondria. The specified cells were harvested as per the manufacturer's experimental procedure, rinsed with PBS, and incubated with 0.5 mL of JC-1 solution for 20 min. After centrifugation at 300 g for 3 min, the cells were washed twice with JC-1 buffer (1×), and then resuspended in 500 μL of JC-1 buffer (1×) for mitochondrial membrane potential analysis using flow cytometry (NovoCyte, Agilent, USA).

Immunofluorescent assessment of BHLHE40 expression in HEI-OC1 cells

Cell climbing sheets were fixed in 4% paraformaldehyde (80096618, Sinoreagen, Shanghai, China) for 15 min and permeabilized with 0.1% tritonX-100 (ST795, Beyotime, Shanghai, China) for 30 min at room temperature. Following three washes with PBS, the specimens were sealed with 1% bovine serum albumin (BSA; A602440-0050, Sangon, Shanghai, China) for 15 min at 25°C. Subsequently, they were incubated with the primary antibody anti-BHLHE40 (1: 100; 17895-1-AP, Proteintech Group, Inc., Wuhan, China) at 4°C overnight. And a secondary Cy3-Goat Anti-Rabbit IgG antibody (1: 200; SA00009-2, Proteintech Group, Inc., Wuhan, China) was then applied under darkness at a concentration of 1:200 for 60 min. DAPI was used for nuclear re-stain. Following a rinsing in PBS, fluorescent visualization of HEI-OC1 cells was performed on a BX53 microscope (Olympus, Tokyo, Japan) with the DP73 photography system.

β-galactosidase staining

The activity levels of senescence-associated β-galactosidase (SA-β-gal), a marker of cellular senescence, were confirmed by a β-galactosidase staining kit (G1580, Solarbio, Beijing, China) according to the standard experimental procedure from manufacturer. Briefly, HEI-CO1 cells were fixed with 1 mL β-gal fixative for 15 min at 25°C, followed by incubation with 1 mL staining solution at 37°C overnight. Brightfield

images were taken at 100× magnification using an Olympus IX53 microscope (OLYMPUS, Tokyo, Japan).

Dual-luciferase reporter assay

To investigate the potential regulatory of BHLHE40 on *Hdac2* transcriptional activity, the luciferase reporter plasmid containing *Hdac2* promoter region from −1000 to +100 relative to the transcription start site was constructed by inserting nucleotide fragments into the vector. For the luciferase activity assay, HEK293 cells were co-transfected with this luciferase reporter plasmid, *Bhlhe40* overexpressing plasmid, and pRL-TK plasmid (KeyGen Biotech) with renilla luciferase gene. Forty-eight hours later, the luciferase activity was measured using the Luciferase Assay Kit (KGAF040, KeyGen Biotech, Nanjing, China) according to the manufacturer's protocol.

Statistical analysis

The experiments were conducted in triplicate, with all values presented as the mean ± standard deviation (SD). Statistical analysis was performed using unpaired student's *t*-test for comparisons between two groups and ordinary one-way ANOVA for comparisons among multiple groups. A *p*-value of less than 0.05 was considered statistically significant.

Results

Bhlhe40 was downregulated in H_2O_2-treated HEI-OC1 cells

The results depicted in Figs. 1A and 1B demonstrated that HEI-OC1 cells, when exposed to 2 mM H_2O_2 for 4, 8, and 12 h, exhibited a time-dependent pattern of cell death. Further flow cytometry analysis revealed that the exposure to 2 mM H_2O_2 led to a significant increase in apoptotic cells, with 31.91% at 8 h and 47.97% at 12 h (Figs. 1C and 1D). Additionally, a decrease in *Bhlhe40* expression was observed in a time-dependent manner following H_2O_2 treatment, particularly evident after 8 h (Figs. 1E and 1F). Immunofluorescent assay results further supported this finding, showing a noticeable reduction in *Bhlhe40* levels in HEI-OC1 cells exposed to 2 mM H_2O_2 for 8 h (Fig. 1G).

Overexpression of Bhlhe40 inhibited H_2O_2-triggered HEI-OC1 cell apoptosis

To investigate the relationship between H_2O_2-induced apoptosis of HEI-OC1 cells and the expression of *Bhlhe40*, a *Bhlhe40* overexpressing HEI-OC1 cell line was generated using the pDC315 adenoviral vector system (Fig. 2A). The efficiency of *Bhlhe40* overexpression was confirmed by real-time PCR and western blotting assay (Figs. 2B and 2C).

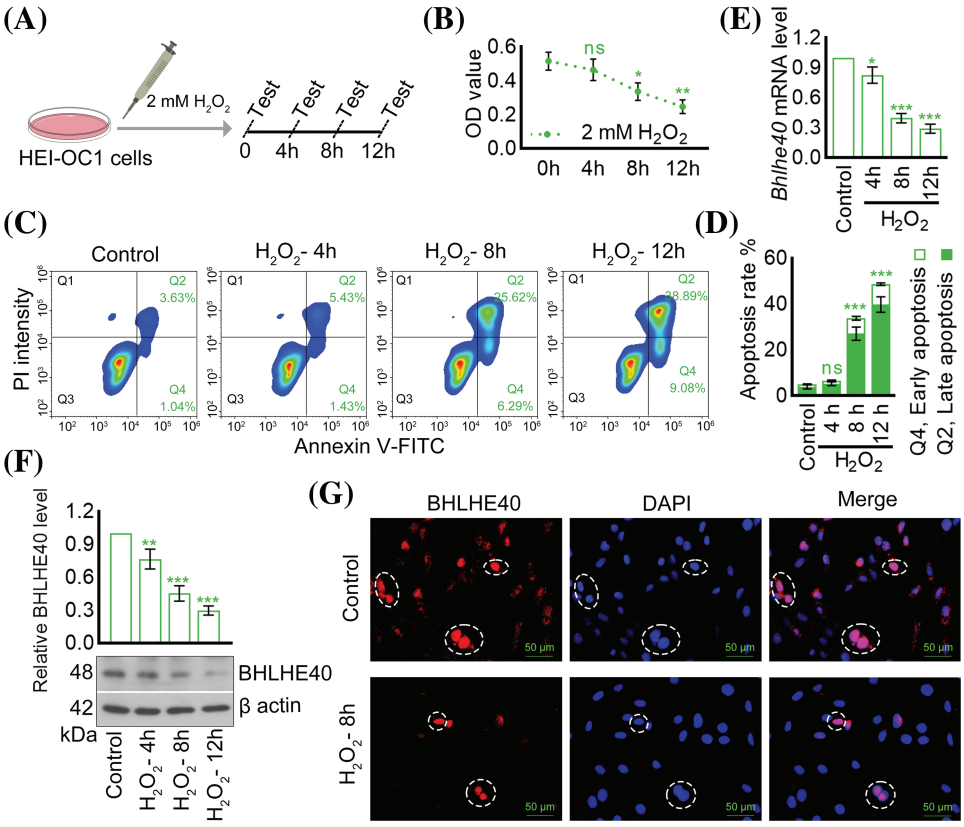

FIGURE 1. H_2O_2 treatment resulted in the downregulation of *Bhlhe40* in HEI-OC1 cells. (A) HEI-OC1 cells were exposed to 2 mM H_2O_2 for specified durations. (B) Cell viability was assessed using the CCK-8 assay. (C and D) Apoptosis was measured though flow cytometry. (E and F) The mRNA and protein levels of *Bhlhe40* were determined via real-time PCR and western blotting, respectively, with corresponding gray value analysis of the western blotting results. (G) The BHLHE40 expression in HEI-OC1 cells was examined using immunofluorescent assay, with DAPI-labeled nuclei (blue fluorescent) for visualization. n = 3. *$p < 0.05$, **$p < 0.01$ and ***$p < 0.001$ *vs*. Control group, while "ns" indicated no statistical significance.

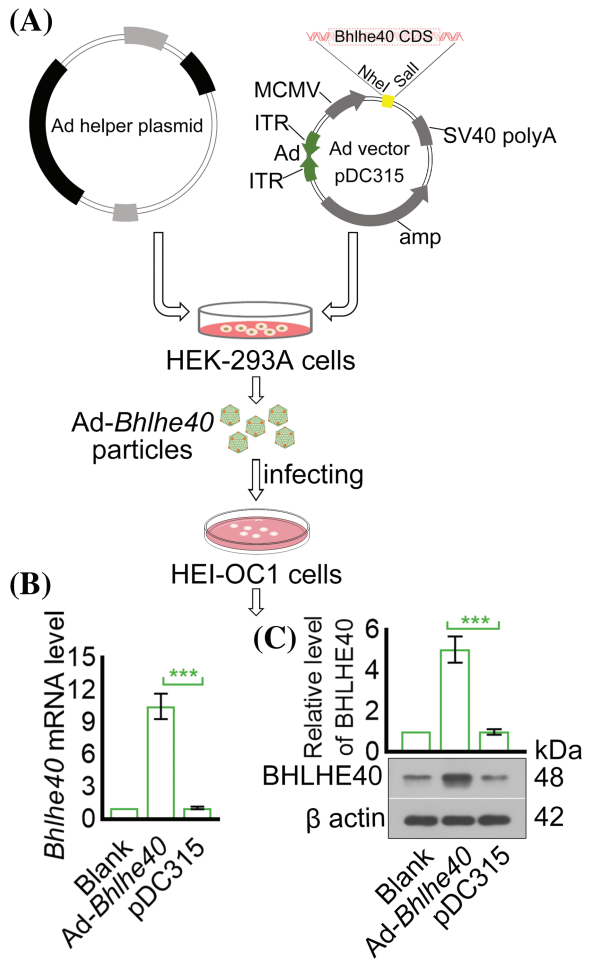

FIGURE 2. Construction of *Bhlhe40* overexpressing HEI-OC1 cells. (A) Construction of recombinant adenovirus. (B and C) The expression of *Bhlhe40* in HEI-OC1 cells were detected by real-time PCR and western blotting, with the gray value of BHLHE40 western blotting result measured. n = 3. ***$p < 0.001$.

Subsequent CCK-8 assay demonstrated a significant reduction in HEI-OC1 cell viability following H_2O_2 exposure, which was rescued by *Bhlhe40* overexpression (Fig. 3A). Flow cytometry analysis indicated that *Bhlhe40* overexpression also hindered H_2O_2-induced cell apoptosis (Figs. 3B and 3C), a finding further supported by followed TUNEL assays (Fig. 3D). Furthermore, activity detection revealed that H_2O_2 treatment led to an increase in Caspase-3 activity, which was counteracted by *Bhlhe40* overexpression (Fig. 3E).

Overexpression of Bhlhe40 reduced H_2O_2-triggered oxidative stress and mitochondrial injury

Subsequent analysis showed that the oxidative stress markers SOD, CAT and GPx were notably reduced in HEI-OC1 cells after exposure to H_2O_2 (Figs. 4A–4C). Conversely, *Bhlhe40* overexpression enhanced the activity of SOD, CAT and GPx (Figs. 4A–4C). Additionally, DHE probe detection indicated that *Bhlhe40* overexpression alleviated the generation of ROS induced by H_2O_2 (Fig. 4D). Furthermore, JC-1 analysis revealed that H_2O_2 treatment led to a decrease in mitochondrial membrane potential, which represented the accelerated apoptosis. Nevertheless, this effect was reversed by *Bhlhe40* overexpression (Fig. 4E).

Overexpression of Bhlhe40 delayed H_2O_2-triggered cell senescence

The SA-β-gal staining showed that *Bhlhe40* overexpression suppressed H_2O_2-induced cell senescence, as evidenced by a decrease in the number of SA-β-gal-positive HEI-OC1 cells (Fig. 5A). Besides, the expression of P53, P21 and P16 was assessed in HEI-OC1 cells. As depicted in Fig. 5B, the elevated levels of P53, P21 and P16 were observed in cells exposed to H_2O_2 but decreased after *Bhlhe40* overexpression.

Overexpression of Bhlhe40 inhibited the transcription of Hdac2

Histone acetylation has been previously identified as playing a role in the pathogenesis of noise-induced cochlear cell death and hearing loss [23]. In this study, we explored the effects of *Bhlhe40* on the expression of histone deacetylases 1, 2, and 3 (*Hdac1*, *Hdac2* and *Hdac3*). Our findings demonstrated that *Bhlhe40* overexpression led to the inhibition of H_2O_2-induced *Hdac2* expression, while not

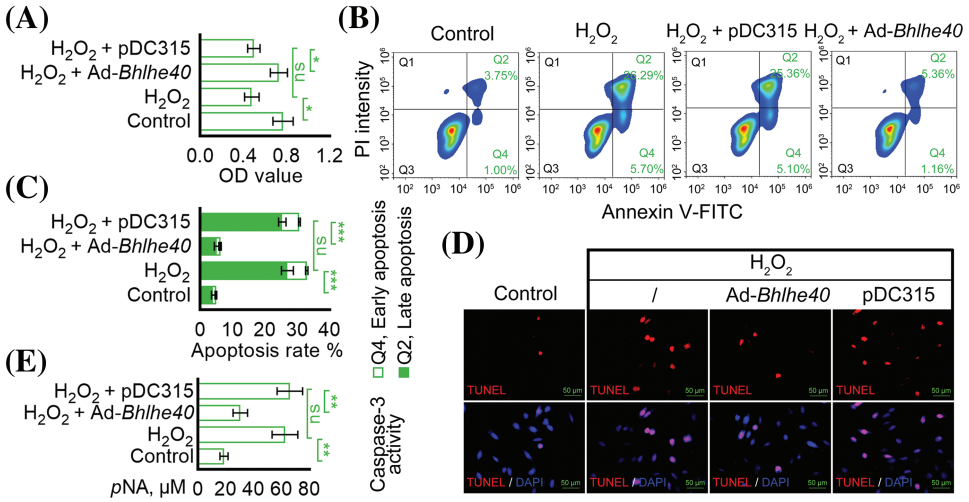

FIGURE 3. Overexpression of *Bhlhe40* inhibited H_2O_2-induced HEI-OC1 cell apoptosis. (A) Cell viability was assessed using the CCK-8 assay. (B and C) Apoptosis was detected by flow cytometry. (D) TUNEL apoptotic assay: TUNEL-positive nuclei (red fluorescent) represent apoptotic cells. DAPI-labeled nuclei (blue fluorescent). (E) Caspase-3 activity assay n = 3. *$p < 0.05$, **$p < 0.01$ and ***$p < 0.001$, while "ns" indicated no statistical significance.

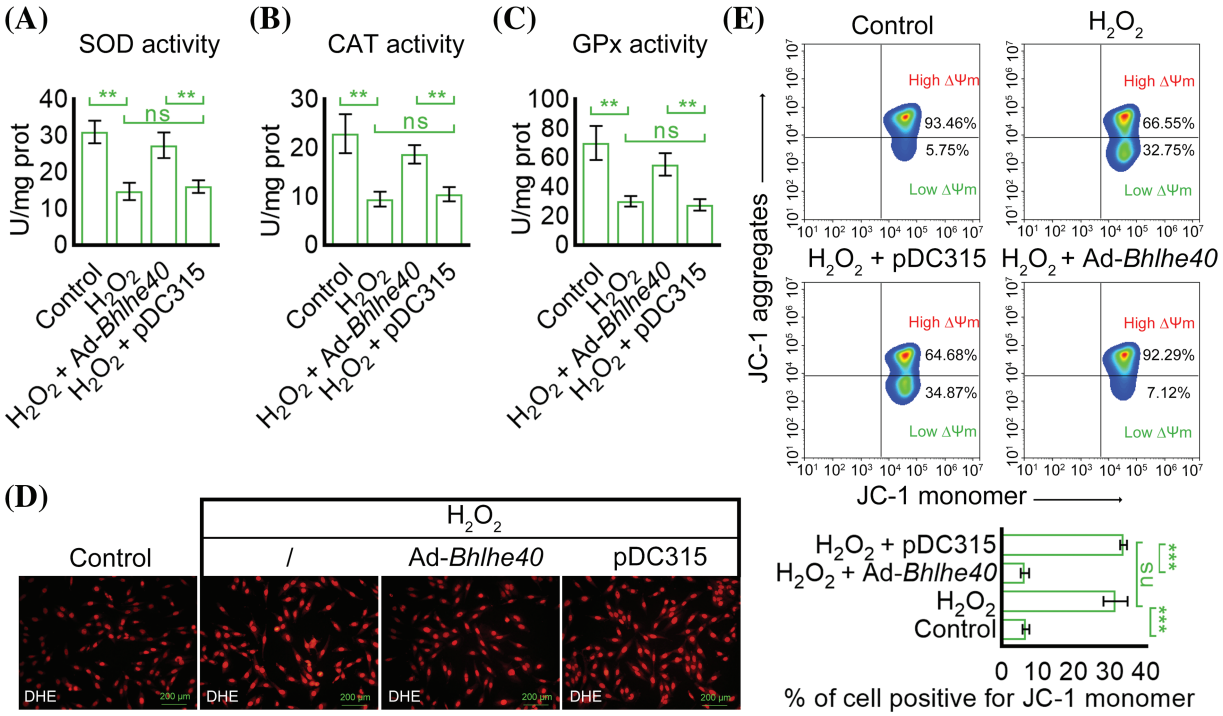

FIGURE 4. Overexpression of *Bhlhe40* reduced H_2O_2-induced oxidative stress and mitochondrial membrane potential decrease in HEI-OC1 cells. (A–C) Detection of the activity of oxidative stress markers: SOD, CAT and GPx, respectively. (D) ROS detection with the DHE probe (red fluorescent). (E) The ΔΨm in mitochondrion was analyzed by the corresponding kit and flow cytometry. n = 3. $^{**}p < 0.01$ and $^{***}p < 0.001$, while "ns" indicated no statistical significance.

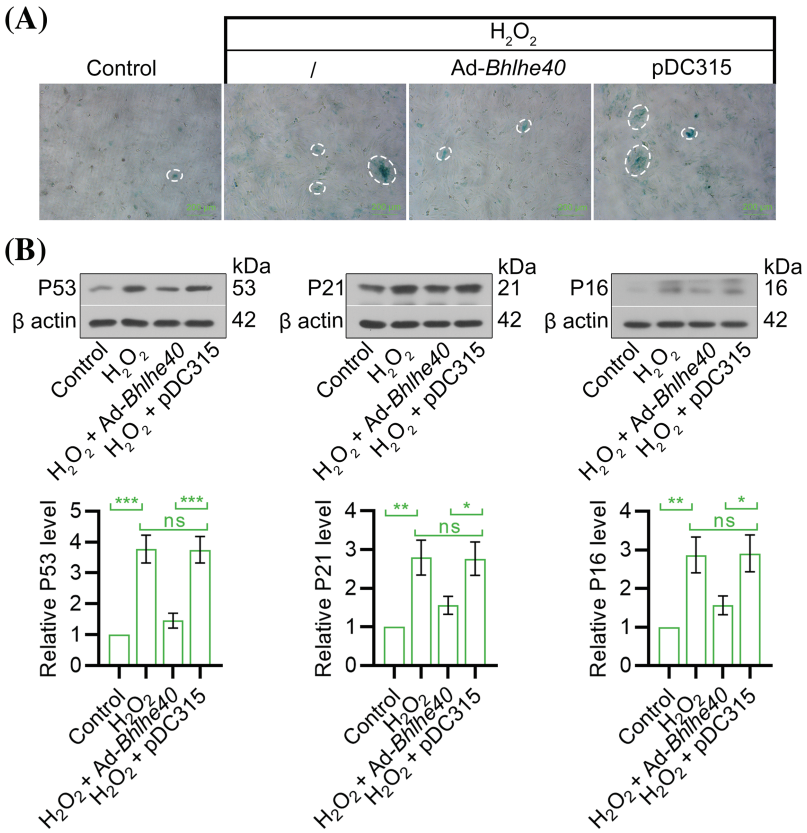

FIGURE 5. Overexpression of *Bhlhe40* alleviated H_2O_2-induced HEI-OC1 cell senescence. (A) Cell senescence was evaluated by the SA-β-Gal staining. (B) The expression of senescence-associated factors (P53, P21 and P16) were detected by western blotting, with corresponding gray value analysis presented n = 3. $^{*}p < 0.05$, $^{**}p < 0.01$ and $^{***}p < 0.001$, while "ns" indicated no statistical significance.

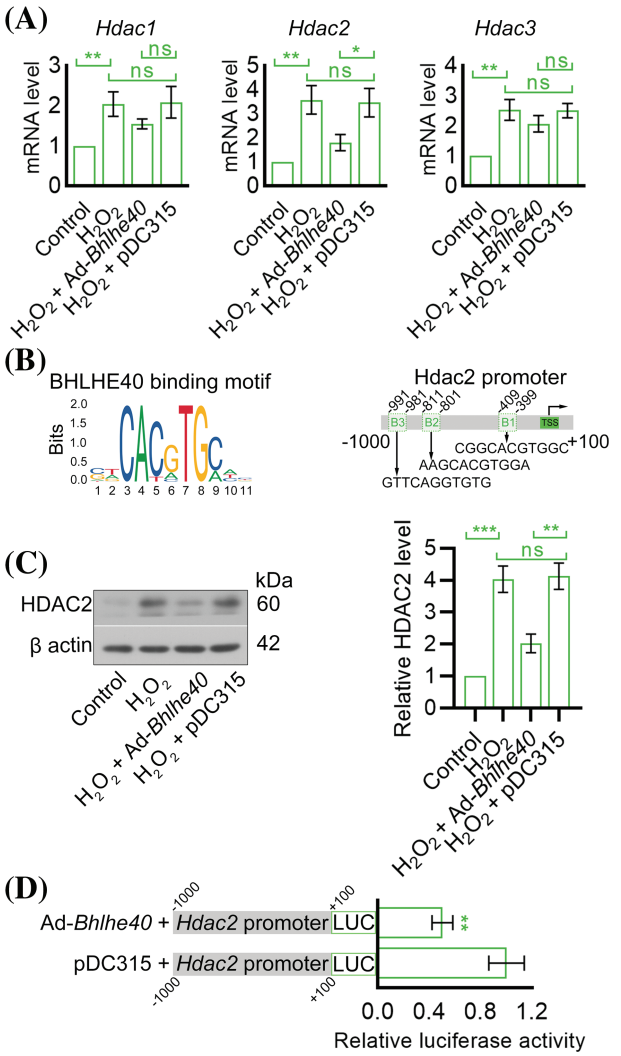

FIGURE 6. Overexpression of *Bhlhe40* curtailed the transcription of *Hdac2*. (A) The mRNA levels of *Hdac1*, *Hdac2* and *Hdac3* in HEI-OC1 cells were detected by real-time PCR. (B) The BHLHE40-binding motif (obtained from JASPAR database) and three potential BHLHE40-responsive elements (B1, B2 and B3) with the JASPAR Score > 8.0 were identified in *Hdac2* promoter region. (C) HDAC2 expression in HEI-OC1 cells was detected by western blotting and quantified by grayscale analysis. (D) The *Hdac2* promoter activity was determined using a dual-luciferase reporter assay. n = 3. *$p < 0.05$, **$p < 0.01$ and ***$p < 0.001$, while "ns" indicated no statistical significance.

significantly affecting the mRNA levels of *Hdac1* and *Hdac3* (Fig. 6A). Utilizing the JASPAR online database (http://jaspar.genereg.net/), we identified 3 potential BHLHE40-responsive elements in the promoter region of *Hdac2* (Fig. 6B). Further western blot analysis confirmed that *Bhlhe40* overexpression suppressed the expression of HDAC2 protein (Fig. 6C), possibly due to the repression of *Hdac2* transcription (Fig. 6D).

Discussion

Noise-or drug-induced insults often leads to hearing loss, which is typically associated with damage to cochlear hair cells [3,4]. Given that damaged hair cells in mammals are irreversible [24], understanding the mechanisms implicated in cochlear hair cell injury could be crucial in developing treatments for hearing loss. Oxidative stress has been identified as a key factor in damaging cochlear hair cells, and further contributing to the development of acquired hearing loss [3]. Recently, H_2O_2 has been commonly used to induce the pathological models of hearing loss caused by various factors, including age-related hearing loss [25] and noise-induced hearing loss [26]. Therefore, H_2O_2 was employed in this study to induce injury to cochlear hair cells. The salient results of this research indicate that the downregulation of *Bhlhe40* was observed in HEI-OC1 cells treated with H_2O_2. Furthermore, the overexpression of *Bhlhe40* was found to inhibit H_2O_2-induced cell apoptosis, oxidative stress, and senescence. These effects may be mediated at least in part by the repression of *Hdac2* transcription.

Bhlhe40 participates in many crucial processes during differentiation of various cell lineages [27]. Data from the Gene Expression Omnibus (GEO) database (https://www.ncbi.nlm.nih.gov/geo/) revealed a significant downregulation of *Bhlhe40* in cisplatin-induced mouse cochlear hair cells. Consistent with these findings, our study observed similar results in H_2O_2-treated HEI-OC1 cells. The regulatory transcription factors of cochlear hair cell regeneration show promise for restoring hearing function. Recent research using single-cell RNA sequencing of adult mouse cochlear hair cells identified multiple key transcriptional regulators, including *Bhlhe40*, that promoted the transition of hair cells to a more mature outer hair cell-like state [28]. Our investigation demonstrated that *Bhlhe40* overexpression effectively inhibited H_2O_2-triggered HEI-OC1 cell apoptosis. ROS is regarded as harmful byproduct of cellular metabolism [29], with its overproduction and subsequent apoptosis induction has been shown to be an important contributor to some types of sensorineural hearing loss [30,31]. Antioxidant enzymes like SOD, CAT, and GPx are capable of reducing ROS levels to alleviate oxidative stress [32]. Encouragingly, our results showed that *Bhlhe40* overexpression restored the decline in SOD, CAT and GPx activities and the increase in ROS levels caused by H_2O_2, indicating a protective role of *Bhlhe40* against H_2O_2-induced oxidative stress in HEI-OC1 cells. Furthermore, we demonstrated that *Bhlhe40* overexpression delayed H_2O_2-induced cell senescence, as evidenced by the reversal of upregulated P53, P21 and P16 levels in treated HEI-OC1 cells.

As a transcriptional repressor, *Bhlhe40* represses the transcription of specific genes involved in cell growth and terminal differentiation via both *Hdac*-dependent and *Hdac*-independent mechanisms [33]. A previous study showed that *Hdac1*, *Hdac2* and *Hdac3* were all increased in the cochlear cells of mice exposure to the traumatic noise [21]. Similarly, our study observed upregulation of *Hdac1*, *Hdac2* and *Hdac3* in HEI-OC1 cells treated with H_2O_2. Interestingly, overexpression of *Bhlhe40* was able to reverse the elevated levels of *Hdac2* level but not *Hdac1* or *Hdac3*.

This suggested a potential role of *Bhlhe40* in repressing of *Hdac2* transcription. The JASPAR online database identified BHLHE40-responsive elements in the promoter region of *Hdac2*, which was further confirmed by a luciferase reporter assay demonstrating affinity of BHLHE40 for the Hdac2 promoter region. Previous studies have indicated that treatment with *Hdac* inhibitors like Trichostatin A or Vorinostat can effectively alleviate ototoxic drug-induced damage or noise-induced loss of outer hair cells, thus preventing hearing loss [21,34]. This study examined the negative regulation of *Bhlhe40* on *Hdac2*, however, further investigation is needed to determine if *Hdac2* transcriptional repression plays a role in the beneficial impact of *Bhlhe40* on cochlear hair cell injury.

Taken together, the current study illustrated that *Bhlhe40* has the ability to inhibit H_2O_2-induced cell apoptosis, oxidative stress, and senescence in HEI-OC1 cells. This study is the first to uncover the impacts of *Bhlhe40*, as well as the regulation of *Bhlhe40* on *Hdac2* in an H_2O_2-induced oxidative injury model in cochlear hair cells. These findings lend support to the potential development of a targeted therapy for hearing loss that leverages the molecular mechanism involving *Bhlhe40*. Moving forward, it is considered that additional investigations be carried out using an *in vivo* animal model to further explore the role of *Bhlhe40* in cochlear hair cell injury and the expression levels of *Hdac2*.

Acknowledgement: None.

Funding Statement: This research was supported by the Special Fund for Economic and Technological Development of Longgang District, Shenzhen (LGKCYLWS2021000030).

Author Contributions: The authors confirm contribution to the paper as follows: study conception and design: Xianhai Zeng; data collection: Liting Wen, Xiaoxia Zeng, Peixiong Chen, Yangyang Li; analysis and interpretation of results: Liting Wen, Xiaoxia Zeng; draft manuscript preparation: Xianhai Zeng, Liting Wen, Dapeng Zhao. All authors reviewed the results and approved the final version of the manuscript.

Availability of Data and Materials: The datasets generated during and/or analyzed during the current study are available from the corresponding author on reasonable request.

Ethics Approval: Not applicable.

Conflicts of Interest: The authors declare that they have no conflicts of interest to report regarding the present study.

References

1. Youm I, Li W. Cochlear hair cell regeneration: an emerging opportunity to cure noise-induced sensorineural hearing loss. Drug Discov Today. 2018;23(8):1564–9. doi:10.1016/j.drudis.2018.05.001.
2. Quan YZ, Wei W, Ergin V, Rameshbabu AP, Huang M, Tian C, et al. Reprogramming by drug-like molecules leads to regeneration of cochlear hair cell-like cells in adult mice. Proc Natl Acad Sci U S A. 2023;120(17):e2215253120. doi:10.1073/pnas.2215253120.
3. Wu F, Xiong H, Sha S. Noise-induced loss of sensory hair cells is mediated by ROS/AMPKα pathway. Redox Biol. 2020;29:101406. doi:10.1016/j.redox.2019.101406.
4. Han WJ, Shi XR, Nuttall A. Noise-induced nitrotyrosine increase and outer hair cell death in guinea pig cochlea. Chin Med J. 2013;126(15):2923–7. doi:10.3760/cma.j.issn.0366-6999.20130838.
5. Zhang J, Zhao Y, Tian Y, Geng M, Liu Y, Zhang W, et al. Genome-wide screening in the haploid system reveals *Slc25a43* as a target gene of oxidative toxicity. Cell Death Dis. 2022;13(3):284. doi:10.1038/s41419-022-04738-4.
6. Fetoni AR, Paciello F, Rolesi R, Paludetti G, Troiani D. Targeting dysregulation of redox homeostasis in noise-induced hearing loss: oxidative stress and ROS signaling. Free Radic Biol Med. 2019;135:46–59. doi:10.1016/j.freeradbiomed.2019.02.022.
7. Waqas M, Gao S, us Iram S, Ali MK, Ma Y, Li W. Inner ear hair cell protection in mammals against the noise-induced cochlear damage. Neur Plast. 2018;2018:1–9. doi:10.1155/2018/3170801.
8. Li M, Chen D, Ke J, Zheng R, Su J, Zheng Z, et al. Inhibition of H_2O_2-induced apoptosis of GC2-spg cells by functionalized selenium nanoparticles with lentinan through ROS-mediated ERK/p53 signaling pathways. BIOCELL. 2023;47(2):401–8. doi:10.32604/biocell.2023.025154.
9. Zhao T, Liu X, Sun Z, Zhang J, Zhang X, Wang C, et al. RNA-seq analysis of potential lncRNAs for age-related hearing loss in a mouse model. Aging. 2020;12(8):7491–510. doi:10.18632/aging.103103.
10. Chen GD, Daszynski DM, Ding D, Jiang H, Woolman T, Blessing K, et al. Novel oral multifunctional antioxidant prevents noise-induced hearing loss and hair cell loss. Hear Res. 2020;388:107880. doi:10.1016/j.heares.2019.107880.
11. Pisani A, Paciello F, Montuoro R, Rolesi R, Galli J, Fetoni AR. Antioxidant therapy as an effective strategy against noise-induced hearing loss: from experimental models to clinic. Life. 2023;13(4):1035. doi:10.3390/life13041035.
12. Tsuyama T, Sato Y, Yoshizawa T, Matsuoka T, Yamagata K. Hypoxia causes pancreatic β-cell dysfunction and impairs insulin secretion by activating the transcriptional repressor BHLHE40. EMBO Rep. 2023;24(8):e56227. doi:10.3390/ijms25084186.
13. Kiss Z, Mudryj M, Ghosh PM. Non-circadian aspects of BHLHE40 cellular function in cancer. Genes Cancer. 2020;11(1–2):1–19. doi:10.3389/fcell.2021.644346.
14. Wesolowski L, Ge J, Castillon L, Sesia D, Dyas A, Hirosue S, et al. The SWI/SNF complex member SMARCB1 supports lineage fidelity in kidney cancer. iScience. 2023;26(8):107360. doi:10.1016/j.isci.2023.107360.
15. Zhao L, Liu D, Ma W, Gu H, Wei X, Luo W, et al. Bhlhe40/Sirt1 axis-regulated mitophagy is implicated in all-*trans* retinoic acid-induced spina bifida aperta. Front Cell Dev Biol. 2021;9:644346. doi:10.1038/s41419-021-04473-2.
16. Zhong G, Mercado MAB, Li Q, Quick CM, Kim Y, Palmer R, et al. BHLHE40 drives protective polyfunctional CD4 T cell differentiation in the female reproductive tract against *Chlamydia*. PLoS Pathog. 2024;20(1):e1011983. doi:10.1371/journal.ppat.1011983.
17. Vercherat C, Chung TK, Yalcin S, Gulbagci N, Gopinadhan S, Ghaffari S, et al. Stra13 regulates oxidative stress mediated skeletal muscle degeneration. Hum Mol Genet. 2009;18(22):4304–16. doi:10.1128/MCB.00387-15.

18. Bek MJ, Wahle S, Müller B, Benzing T, Huber TB, Kretzler M, et al. Stra13, a prostaglandin E_2-induced gene, regulates the cellular redox state of podocytes. Faseb J. 2003;17(6):682–4. doi:10.1016/j.trsl.2007.01.002.
19. Defourny J, Aghaie A, Perfettini I, Avan P, Delmaghani S, Petit C. Pejvakin-mediated pexophagy protects auditory hair cells against noise-induced damage. Proc Natl Acad Sci U S A. 2019; 116(16):8010–7. doi:10.1073/pnas.1821844116.
20. Ivanova AV, Ivanov SV, Danilkovitch-Miagkova A, Lerman MI. Regulation of STRA13 by the von Hippel-Lindau tumor suppressor protein, hypoxia, and the UBC9/ubiquitin proteasome degradation pathway. J Biol Chem. 2001;276(18): 15306–15. doi:10.1136/jmg.2004.029835.
21. Chen J, Hill K, Sha SH. Inhibitors of histone deacetylases attenuate noise-induced hearing loss. J Assoc Res Otolaryngol. 2016;17(4):289–302. doi:10.1007/s10162-016-0567-7.
22. Kalinec GM, Park C, Thein P, Kalinec F. Working with auditory HEI-OC1 Cells. J Vis Exp. 2016;(115):54425. doi:10.3791/54425.
23. Xie L, Zhou Q, Chen X, Du X, Liu Z, Fei B, et al. Elucidation of the Hdac2/Sp1/*miR-204-5p/Bcl-2* axis as a modulator of cochlear apoptosis via *in vivo*/*in vitro* models of acute hearing loss. Mol Ther-Nucleic Acids. 2021;23:1093–109. doi:10.1016/j.omtn.2021.01.017.
24. Shibata SB, West MB, Du X, Iwasa Y, Raphael Y, Kopke RD. Gene therapy for hair cell regeneration: review and new data. Hear Res. 2020;394:107981. doi:10.1016/j.heares.2020.107981.
25. Li L, Xu K, Bai X, Wang Z, Tian X, Chen X. UCHL1 regulated by Sp1 ameliorates cochlear hair cell senescence and oxidative damage. Exp Ther Med. 2023;25(2):94. doi:10.3892/etm.2023.11793.
26. Yang H, Zhu Y, Ye Y, Guan J, Min X, Xiong H. Nitric oxide protects against cochlear hair cell damage and noise-induced hearing loss through glucose metabolic reprogramming. Free Radic Biol Med. 2022;179(2):229–41. doi:10.1016/j.freeradbiomed.2021.11.020.
27. Boudjelal M, Taneja R, Matsubara S, Bouillet P, Dolle P, Chambon P. Overexpression of Stra13, a novel retinoic acid-inducible gene of the basic helix-loop-helix family, inhibits mesodermal and promotes neuronal differentiation of P19 cells. Genes Dev. 1997;11(16):2052–65. doi:10.1101/gad.11.16.2052.
28. Tu S, Zuo J. Systematic single cell RNA sequencing analysis reveals unique transcriptional regulatory networks of Atoh1-mediated hair cell conversion in adult mouse cochleae. PLoS One. 2023;18(12):e0284685. doi:10.1371/journal.pone.0284685.
29. Jomova K, Raptova R, Alomar SY, Alwasel SH, Nepovimova E, Kuca K, et al. Reactive oxygen species, toxicity, oxidative stress, and antioxidants: chronic diseases and aging. Arch Toxicol. 2023;97(10):2499–574. doi:10.1007/s00204-023-03562-9.
30. Rousset F, Nacher-Soler G, Coelho M, Ilmjarv S, Kokje VBC, Marteyn A, et al. Redox activation of excitatory pathways in auditory neurons as mechanism of age-related hearing loss. Redox Biol. 2020;30:101434. doi:10.1016/j.redox.2020.101434.
31. Zhao Z, Han Z, Naveena K, Lei G, Qiu S, Li X, et al. ROS-responsive nanoparticle as a berberine carrier for OHC-targeted therapy of noise-induced hearing loss. ACS Appl Mater Interf.. 2021;13(6):7102–14. doi:10.1021/acsami.0c21151.
32. Mosa KA, El-Naggar M, Ramamoorthy K, Alawadhi H, Elnaggar A, Wartanian S, et al. Copper nanoparticles induced genotoxicty, oxidative stress, and changes in superoxide dismutase (SOD) gene expression in cucumber (*Cucumis sativus*) plants. Front Plant Sci. 2018;9:872. doi:10.3389/fpls.2018.00872.
33. Sun H, Taneja R. Stra13 expression is associated with growth arrest and represses transcription through histone deacetylase (HDAC)-dependent and HDAC-independent mechanisms. Proc Natl Acad Sci U S A. 2000;97(8):4058–63. doi:10.1073/pnas.070526297.
34. Chen FQ, Schacht J, Sha SH. Aminoglycoside-induced histone deacetylation and hair cell death in the mouse cochlea. J Neurochem. 2009;108(5):1226–36. doi:10.1111/j.1471-4159.2009.05871.x.